PAPER

Ultrasensitive surface-enhanced Raman scattering nanosensor for mercury ion detection based on functionalized silver nanoparticles†

Lingxin Chen,*[a] Nan Qi,[ab] Xiaokun Wang,[ac] Ling Chen,[ad] Huiyan You*[b] and Jinhua Li[a]

In this work, a simple, rapid and ultrasensitive surface-enhanced Raman scattering (SERS) nanosensor was developed for mercury ion (Hg^{2+}) detection based on 4-mercaptopyridine (4-MPY) functionalized silver nanoparticles (AgNPs) (4-MPY-AgNPs) in the presence of spermine. Here, the spermine would bind AgNPs through Ag–N bonds and induce remarkable aggregation of AgNPs, and thereby would generate significantly enhanced Raman intensity of the reporter molecule 4-MPY. Followed by the addition of Hg^{2+}, the formation of the Hg–Ag alloy blocked the adsorption of 4-MPY and spermine, resulting in the dispersion of 4-MPY-AgNPs and thus decreasing the Raman intensity, by which the Hg^{2+} could be sensed by SERS. A good linearity was obtained in the range of 1–100 nM ($R^2 = 0.987$), and the relative standard deviation was between 0.85 and 5.50%. The spermine-induced accumulation of 4-MPY-AgNPs largely enhanced the SERS responses, leading to a high detectability up to 0.34 nM. A real water sample with spiked Hg^{2+} was also analyzed, presenting satisfactory recoveries ranging from 94.5 to 108.5%, confirming the practicability of the SERS nanosensor based method.

1. Introduction

Contamination by heavy metals ions has become a serious threat to the environment and living organisms. Among various heavy metals, mercury ions (Hg^{2+}) are of great concern, since they possess highly toxic and bioaccumulative properties and widely exist in living environments, such as surface water, air, and soil.[1] Excess uptake of Hg^{2+} tends to cause brain, heart, kidney, and lung damage and other chronic diseases.[2,3] The United States Environmental Protection Agency (EPA) has mandated an upper limit of 2 ppb (10 nM) for Hg^{2+} in drinking water. Therefore, high sensitive identification and measurement of Hg^{2+} in aquatic ecosystem has become critically necessary.

In the last few years, various methods for available detection of Hg^{2+} have been developed.[4–10] The traditional detection techniques include atomic emission,[4] atomic absorption,[6] atomic fluorescence,[7] and inductively coupled plasma mass spectrometries.[8] However, most of them are confronted with some limitations with respect to complex instruments, procedures or costs. Currently, nanomaterials, of various sizes, shapes, and compositions, especially, gold nanoparticles (AuNPs) and silver nanoparticles (AgNPs) have been widely used for construction of nanosensors, since they often exhibit high extinction coefficient in the visible region and unique color-tunable behavior that mainly depend on the interparticle distance.[11–14] In recent years, several groups have proposed various detection methods for Hg^{2+} based on AuNPs and AgNPs. Liu's group has developed a one-step, room temperature, colorimetric method by using oligonucleotide-tethered AuNPs probes and a linker oligonucleotide with a number of T–T mismatches, resulting in the formation of particle aggregates accompanied colorimetric response with the addition of Hg^{2+} into the solution.[15] Rex *et al.* have provided a sensitive assay through pushing the limits of Hg^{2+} sensors with gold nanorods, taking advantage of the strong affinity between Au and Hg.[16] Our group has also reported blue-to-red colorimetric sensing strategy for Hg^{2+} and Ag^+ *via* redox-regulated surface chemistry of AuNPs.[17] Although the developed colorimetric methods possess good sensitivity and selectivity, it is still highly desirable to explore simpler and more sensitive methods for the detection of Hg^{2+}.

Surface-enhanced Raman scattering (SERS), an ultrasensitive vibrational spectroscopic technique, has attracted lots of attentions due to its evading photobleaching, narrow bandwidth as well as the ability to detection of multiple analytes by a single laser wavelength. Many researches have reported on the SERS theory and it's commonly considered that two primary

[a] Key Laboratory of Coastal Environmental Processes and Ecological Remediation, Shandong Provincial Key Laboratory of Coastal Environmental Processes, Yantai Institute of Coastal Zone Research, Chinese Academy of Sciences, Yantai 264003, China. E-mail: lxchen@yic.ac.cn; Fax: +86 535 2109130; Tel: +86 535 2109130

[b] Environmental and Chemical Engineering College, Dalian University, Dalian 116600, China. E-mail: dlyhy@dicp.ac.cn; Fax: +86 411 87402436; Tel: +86 411 87402440

[c] College of Chemistry and Chemical Engineering, Qufu Normal University, Qufu 273165, China

[d] University of Chinese Academy of Sciences, Beijing 100049, China

† Electronic supplementary information (ESI) available. See DOI: 10.1039/c3ra47492e

mechanisms contribute to the enhancement, long-range electromagnetic enhancement and short-range chemical enhancement.[18–20] Since its discovery in late 1970s, various types of SERS nanoprobes have been developed.[21–25] For example, Zhan's group has provided an AgNPs aggregates-based SERS substrate for sensitive detection of polycyclic aromatic hydrocarbons.[23] Kuang's group has constructed a simple but highly sensitive SERS sensor platform based on a self-assembled gold nanostar dimer for Hg^{2+} detection.[24] Our group has also developed two SERS strategies for highly sensitive detection of As^{3+} ions[21] and trypsin[25] using glutathione functionalized AgNPs and 4-mercaptopyridine (4-MPY)-functionalized AgNPs, respectively.

Inspired by these studies, herein, we proposed to develop a sensitive and selective SERS approach for Hg^{2+} detection based on 4-MPY functionalized AgNPs with the aid of redox-regulated surface chemistry of AgNPs. Spermine could induce the aggregation of 4-MPY functionalized AgNPs through Ag–N bonds,[26] and thus, in the presence of spermine, significant SERS enhancement of Raman report molecule 4-MPY was obtained. However, with the addition of Hg^{2+}, the spermine-induced aggregation was disturbed, which may well be mainly due to that the interaction between Hg^{2+} and AgNPs could occur in a short time.[27] The resultant Hg–Ag alloy on the surface of AgNPs could affect the adsorption of spermine and 4-MPY, and thereby would result in the decreased of Raman signals. Several major influence parameters of the SERS intensity were investigated, and under optimized conditions, excellent analytical performances were attained such as high sensitivity, high precision and high selectivity. The SERS nanosensor method was further demonstrated potentially applicable for monitoring Hg^{2+} in real water samples.

2. Experimental

2.1. Reagents

Silver nitrate ($AgNO_3$, 99.8%) and sodium hydroxide (NaOH, 96%) were obtained from Sinopharm Chemical Reagent Co., Ltd. (Shanghai, China), hydroxylamine hydrochloride ($NH_2OH \cdot HCl$) was purchased from Tianjin Kermel Chemical Reagent Co., Ltd. (Tianjin, China) and used as received. 4-Mercaptopyridine (4-MPY, 95%) and spermine (97%) were obtained from Sigma-Aldrich (USA). Mercury nitrate ($Hg(NO_3)_2$) was purchased from Sinopharm Group Chemical Reagent Co., Ltd. (Beijing, China). All other solvents and reagents used were of analytical grade.

2.2. Instrumentation

SERS spectra were recorded using a Thermo Scientific RFS100 Raman system equipped with a microscope and a 632.8 nm diode pumped He–Ne laser source. The transmission electron microscopy (TEM) analyses were obtained using a JEM-1230 electron microscope (JEOL, Ltd., Japan) operating at 100 kV. Dynamic light scattering (DLS) measurements were performed on a Malvern Zetasizer Nano-ZS90 (ZEN3590, UK). ICP-MS analyses were performed on PerkinElmer Elan DRC II (USA). Solutions throughout the work were prepared using fresh double deionized water, which was produced by a Cascada TM LS Ultrapure water system (Pall Corp., USA) with the water outlet operating at 18.2 MΩ. All glassware in this work were soaked and washed with freshly prepared aqua regia, rinsed thoroughly in double deionized water and dried in air for use.

2.3. Functionalization of AgNPs with 4-MPY

AgNPs were synthesized referring to our previous work[21] with necessary modification by reducing silver nitrate using hydroxylamine hydrochloride at room temperature. First, 1 mL of 0.30 M NaOH solution was added to 89 mL of 1.50 mM $NH_2OH \cdot HCl$ (10.44 mg) solution to maintain an alkaline pH. Next, 10 mL of 0.01 M $AgNO_3$ solution was added to the above solution with continuous stirring. The reaction mixtures were continuously stirred for an additional 0.5 h. The prepared silver colloid was stored at room temperature. Then, 20 μL of 400 μM 4-MPY was added to 2.7 mL of the above prepared silver colloid with stirring for 0.5 h. Finally, the resultant mixtures were 4-MPY functionalized AgNPs (4-MPY-AgNPs).

2.4. SERS detection of Hg^{2+}

20 μL of spermine was added to 100 μL of Tris–HCl buffer solution (pH 8.0, 0.05 mM) containing 4-MPY functionalized AgNPs, and the resultant solutions were incubated for 2 min, followed by adding Hg^{2+} solutions from 10 to 90 μL. The obtained mixtures were incubated at room temperature for 5 min. Then the samples were detected by Raman spectrometry with an exposure time of 4 s.

2.5. Selectivity study

A series of metal ion solutions including Pb^{2+}, Cd^{2+}, K^+, Ca^{2+}, Mg^{2+}, Cu^{2+}, Co^{2+}, Na^+, Mn^{2+}, Cr^{3+}, Fe^{3+}, Zn^{2+} and $MeHg^+$ were prepared and then added to the system to investigate the selectivity of this system toward Hg^{2+} under the same optimized conditions.

2.6. Analysis of real water samples

Tap water samples were collected from our institute and analyzed without treatment. A series of samples were spiked with standard Hg^{2+} solutions at certain concentrations. These spiked samples were added to a 4-MPY functionalized AgNPs containing spermine and 0.05 mM Tris–HCl buffer solution (pH 8.0). The obtained mixtures were incubated at room temperature for 5 min and then measured by SERS.
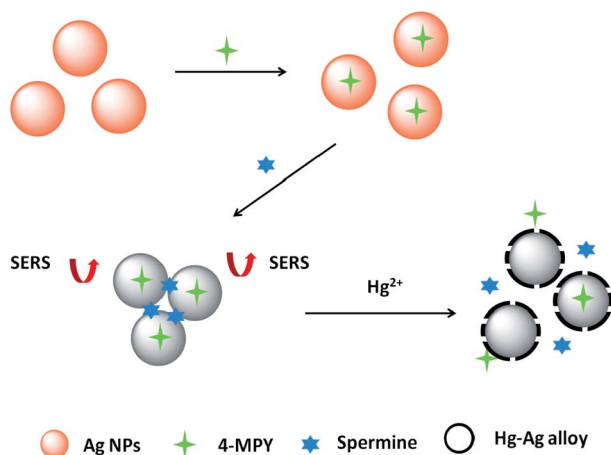
2.7. Safety consideration

Aqua regia has strong oxidizing capacity and adverse effects on human health, thus all of the experiments involving aqua regia should be performed with gloves and protective glasses. The waste solution of the experiment should be collectively reclaimed to avoid polluting the environment.

3. Results and discussion

3.1. Analytical principle

Scheme 1 shows the possible analytical principle of the detection of Hg^{2+} based on SERS by using AgNPs as enhancement substrates. Hydroxylamine chloride ions stabilized AgNPs were well dispersed (Fig. 1A(a)) and presented a bright yellow color (Fig. 1B(a)). In the process of SERS probe synthesis, with the addition of proper amount of Raman reporters 4-MPY, AgNPs were still a bright yellow color (Fig. 1B(b)), which indicated that the 4-MPY functionalized AgNPs remained monodisperse state (Fig. 1A(b)). It was because that 4-MPY replaced parts of the hydroxylamine ions, and then both 4-MPY and hydroxylamine ions were present on the surface of AgNPs. Consequently, 4-MPY functionalized AgNPs could have strong Raman signals, and the presence of hydroxylamine ions could keep the stability of AgNPs. As a rule, 4-MPY combines with AgNPs through three different ways, Ag–S bonds, Ag–N bonds, or via the aromatic π electrons.[25] It could deduce that the 4-MPY molecules adsorbed on the AgNPs surface were mainly through Ag–S bonds, while Ag–N bonds played a minor role and the surface-aromatic π interaction was not very important.[25,28,29] When spermine was added to the 4-MPY-AgNPs solution, remarkable aggregation of the 4-MPY-AgNPs occurred due to the distinctive structure of spermine. Since there are coordinating interactions between N and the electron-deficient surface of the metal nanoparticles, it makes compounds with electron-rich N easily bind onto the surface of metal nanoparticles. Hence, the N-donors have a stronger affinity with AgNPs.[26,30,31] So, in the presence of spermine, the formation of Ag–N bonds led to remarkable aggregation of the 4-MPY-AgNPs (Fig. 1A(c)) along with an obvious color change from bright yellow to brown (Fig. 1B(c)). Meanwhile, the aggregated 4-MPY-AgNPs could produce a number of "hot spots", and therefore the Raman scattering signals of 4-MPY were greatly enhanced (Fig. 2, curve h). However, interestingly, once addition of Hg^{2+} to the system, the SERS signals would be remarkably reduced (Scheme 1) and hence the Hg^{2+} ions could be sensed optically. The redox-regulated surface chemistry between Hg^{2+}
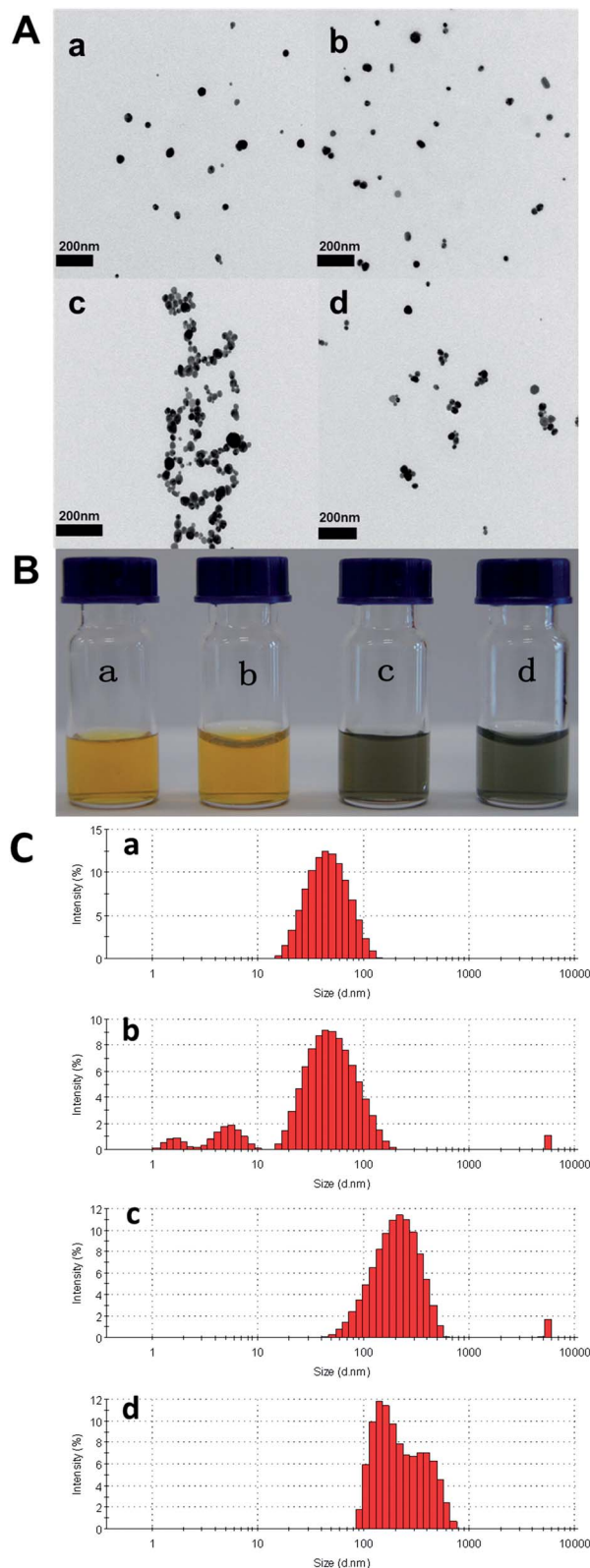

Fig. 1 TEM images (A), color changes (B) and size distributions (C) corresponding to (a) AgNPs, (b) 4-MPY-AgNPs, (c) 4-MPY-AgNPs + spermine, and (d) 4-MPY-AgNPs + spermine + Hg^{2+}.

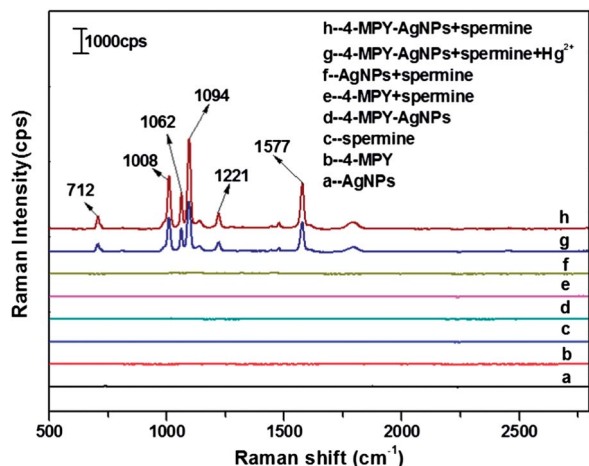Scheme 1 Schematic of the SERS sensing principle for Hg^{2+} detection based on 4-MPY functionalized AgNPs.

Fig. 2   Raman spectra of (a) AgNPs, (b) 4-MPY, (c) spermine, (d) 4-MPY-AgNPs, (e) 4-MPY + spermine, (f) AgNPs + spermine, (g) 4-MPY-AgNPs + spermine + Hg^{2+} and (h) 4-MPY-AgNPs + spermine.

and AgNPs would cause the formation of Hg–Ag alloys and thereby non-uniform Hg–Ag shells would wrap around the AgNPs.[27,32] ICP-MS was used to provide a further evidence for the Hg–Au alloys, as seen in Fig. S1 in the ESI.† Therefore, the adsorption of 4-MPY and spermine on the AgNPs surface was hindered and then it was unfavorable for the aggregation of 4-MPY-AgNPs (Fig. 1A(d)), as illustrated in Scheme 1.

Moreover, the size distributions of particles were measured by dynamic light scattering (DLS). It tends to overestimate the diameters of AgNPs measured by TEM images because DLS measures hydrodynamic diameters of silver nanocomposites.[33] A pronounced difference in the AgNPs at different conditions displayed the different dominant distribution peaks, as shown in Fig. 1C. It was observed that the dominant distribution peak around 50 nm was for AgNPs (a), 57 nm for 4-MPY-AgNPs (b), 222 nm for spermine-induced aggregated 4-MPY-AgNPs (c), and 178 nm for the aggregated 4-MPY-AgNPs with the presence of Hg^{2+} (d), respectively. Even if the DLS signals were spread over a relatively large size distribution, the mean diameter agreed with the mean diameter obtained by TEM. As a result, the aggregation degree could be quantitatively estimated by determining the size distribution by DLS. Consequently, the degree of SERS intensity decrease could be employed for analytical detection of Hg^{2+}.

In order to confirm the feasibility of the SERS sensing for Hg^{2+} detection, a series of control experiments were implemented and the results were shown in Fig. 2. It could be seen that in the presence of separate AgNPs, 4-MPY, spermine, or any two of them, there were no obvious SERS signals (Fig. 2, curve a–f). Excitedly, several strong signal peaks were obtained in the simultaneous presence of AgNPs, 4-MPY (3.0 μM) and spermine (140 μM), as exhibited in Fig. 2 (curve h). However, interestingly, upon addition of Hg^{2+} (10 nM), all SERS peaks significantly decreased (Fig. 2, curve g), which indicated that the formation of Hg–Ag alloy and thereby Hg–Ag shells wrapping around AgNPs destroyed the aggregation of 4-MPY-AgNPs. All the results demonstrated the proposed SERS strategy was feasible to Hg^{2+} analysis.

3.2.   Parameter optimization

In order to acquire satisfactory SERS intensity and thereby analytical results, several parameters were optimized. Firstly, the effect of pH values (pH 7.0–9.0) in 0.05 mM Tris–HCl buffer solution on SERS signal intensity was studied. As seen from Fig. S2A,† the SERS signal was maximized at pH 8.0 and the particles could keep stable, while at pH > 8.0, the SERS signal presented a significant decrease. Thus, a pH 8.0 Tris–HCl buffer solution was selected for the system. Next, the effect of the concentration of 4-MPY on SERS signal intensity was investigated. Six different concentrations of 4-MPY ranging from 1.0 to 3.5 μM were tested, and the corresponding Raman spectra were recorded in Fig. S2B.† It was observed that the SERS signal intensity increased with the concentration increase of 4-MPY, and the largest signal was achieved with 3.0 μM 4-MPY. However, further increasing the concentration of 4-MPY resulted in SERS signal decrease. Thus, the concentration of 3.0 μM was chosen in this work. The influence of the concentration of spermine on the SERS intensity was further investigated. As shown in Fig. S2C,† the spermine at the concentration lower than 140 μM would be less efficient and unfavorable to SERS signals, whereas higher concentration than 140 μM could not induce obvious enhancement of SERS signal. In order to ensure the full combination of AgNPs and spermine, the concentration of 140 μM was adopted.

3.3.   Analytical sensitivity

In order to evaluate the detectability of the developed SERS method, under the above optimized conditions, the SERS spectra of 4-MPY on AgNPs to different concentrations of Hg^{2+} were recorded for sensitivity investigation. As shown in Fig. 3A, there are many spectral features that are characteristics of 4-MPY, such as those at 712, 1008, 1062, 1094, 1221 and 1577 cm^{-1}. It could be clearly seen that the Raman intensity of all the characteristic peaks decreased with the increase of the concentration of Hg^{2+}. The peak at 1094 cm^{-1} corresponding to the ring-breath/C–S stretching mode indicated that 4-MPY was bound to the surface of AgNPs through the S.[34] Also, the 1094 cm^{-1} peak was found to be the most prominent one, and its intensity was very sensitive to the concentration of Hg^{2+}. Therefore, the Raman intensity of 4-MPY on AgNPs at 1094 cm^{-1} was used here for quantitative analysis of Hg^{2+}. As displayed in Fig. 3B, a good linearity was obtained between the Raman intensity and the logarithm of Hg^{2+} concentration within 1–100 nM ($R^2 = 0.987$), with relative standard deviations ranging from 0.85 to 5.50%. The limit of detection based on a signal-to-noise ratio of 3 was estimated to be 0.34 nM, which was lower than the maximum contaminant level for Hg^{2+} in drinking water, namely 10 nM defined by EPA. Therefore, the SERS strategy was indicated highly sensitive and reliable for the detection of Hg^{2+}.

3.4.   Analytical selectivity

In order to demonstrate the analytical selectivity of the SERS system toward Hg^{2+}, other metal ions were introduced for investigation, including Pb^{2+}, Cd^{2+}, K^+, Ca^{2+}, Mg^{2+}, Cu^{2+}, Co^{2+},
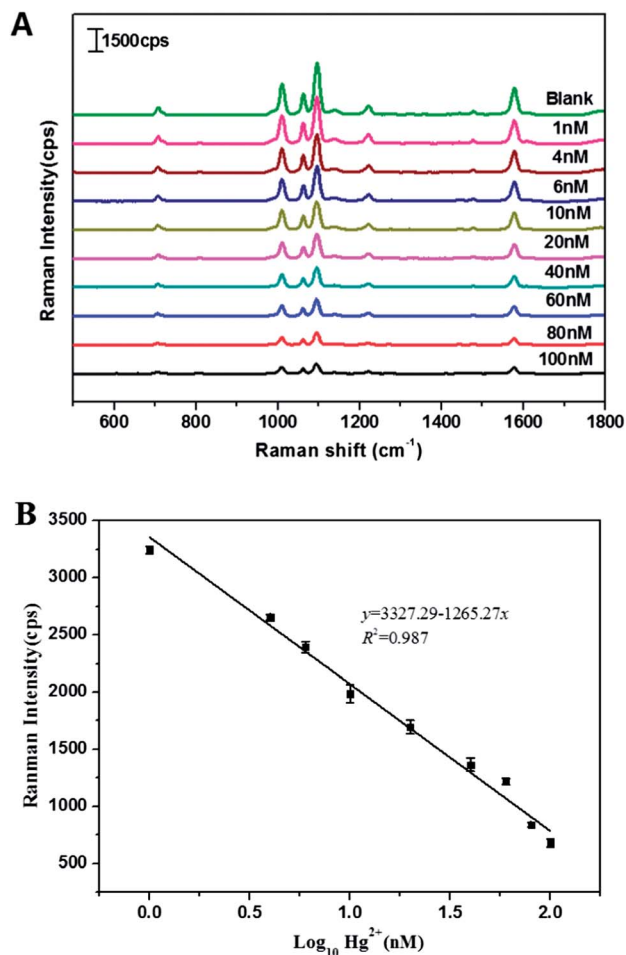
Fig. 3 (A) SERS spectra changes of 4-MPY functionalized AgNPs with different concentrations of Hg^{2+} (0–100 nM). (B) A plot of corresponding intensity of the Raman band at 1094 cm^{-1} *versus* Hg^{2+} concentrations in the range of 1 to 100 nM ($R^2 = 0.987$). The error bars represent the standard deviations based on three independent measurements.

Fig. 4 Relative SERS intensity change of 4-MPY functionalized AgNPs at 1094 cm^{-1} upon the addition of various metal ions. I_0 is the SERS intensity of 4-MPY-AgNPs in the presence of spermine, and I is the SERS intensity in the presence of other metal ions or Hg^{2+}. The concentrations of all the metal ions were individual at 100 nM, except Hg^{2+} at 5 nM, MeHg$^+$ at 10 ppb (46.38 nM).

Table 1 Recoveries of the developed SERS method based on 4-MPY functionalized AgNPs for the detection of Hg^{2+} in tap water samples ($n = 3$)

Sample	Added (nM)	Found (nM) mean ± SD	Recovery (%)
1	2	1.89 ± 0.73	94.50
2	4	4.34 ± 0.34	108.50
3	8	7.96 ± 0.21	99.46
4	10	9.52 ± 1.23	95.34

Na$^+$, Mn^{2+}, Cr^{3+}, Fe^{3+}, Zn^{2+} and MeHg$^+$. As shown in Fig. 4, the SERS intensity ratio presented the maximum value for Hg^{2+}. It was also observed that several other metal ions presented some signals, which was very likely owing to the interaction between the metal ions and 4-MPY as well as the ionic strength effects. Nevertheless, this signal change induced by 100 nM of other metal ions was much smaller comparing with the response to 5 nM Hg^{2+}. Besides, the SERS ratio value for the Hg^{2+} in the presence of a mixture of all the tested other metal ions was found closer to that for the Hg^{2+} individual, as evidenced in Fig. 4. These results indicated that the other metal ions had no significant effect on the Hg^{2+} detection. So, the developed SERS strategy was highly selective toward Hg^{2+}.

3.5. Practical application

To evaluate the application of the presented assay in real samples, we utilized it to analyze Hg^{2+} in tap water samples by using standard addition method. As shown in Table 1, satisfying recoveries were obtai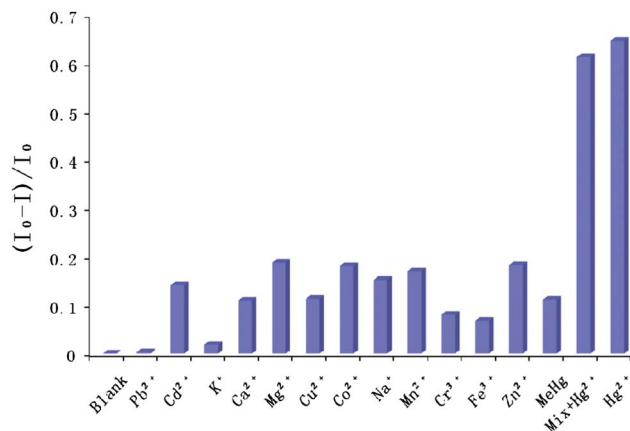ned in a range of 94.5–108.5% for the four spiked concentration levels. The experimental results clearly confirmed that this method was potentially applicable for the detection of Hg^{2+} in real samples.

4. Conclusions

In summary, a simple, rapid, and sensitive SERS nanosensor for detection of Hg^{2+} was developed based on 4-MPY functionalized AgNPs in the presence of spermine. By taking advantage of the redox-regulated surface chemistry between Hg^{2+} and AgNPs, satisfactory analytical performance was obtained. The developed method has a wide linear range (1–100 nM) and a high sensitivity (0.34 nM). In addition, this method exhibited a good selectivity for Hg^{2+} over other interfering metal ions and was successfully applied to analysis of Hg^{2+} in tap water samples. With the appropriate choice of nanomaterials and Raman reporter molecules, especially the smart utilization of specific interactions between targets and substrates, such a sensing strategy can provide great potential for construction of SERS sensors toward various heavy metals.

Acknowledgements

Notes and references

1 J. R. Miller, J. Rowland, P. J. Lechler, M. Desilets and L. C. Hsu, *Water, Air, Soil Pollut.*, 1996, **86**, 373.

2 I. Hoyle and R. D. Handy, *Aquat. Toxicol.*, 2005, **72**, 147.

3 P. B. Tchounwou, W. K. Ayensu, N. Ninashvili and D. Sutton, *Environ. Toxicol.*, 2003, **18**, 149.

4 F. X. Han, W. Dean Patterson, Y. J. Xia, B. B. Maruthi Sridhar and Y. J. Su, *Water, Air, Soil Pollut.*, 2006, **170**, 161.

5 G. Aragay, J. Pons and A. Merkoci, *Chem. Rev.*, 2011, **111**, 3433.

6 J. Gomez-Ariza, F. Lorenzo and T. Garcia-Barrera, *Anal. Bioanal. Chem.*, 2005, **382**, 485.

7 Y. L. Yu, Z. Du and J. H. Wang, *J. Anal. At. Spectrom.*, 2007, **22**, 650.

8 B. Fong, W. Mei, T. S. Siu, J. Lee, K. Sai and S. Tam, *J. Anal. Toxicol.*, 2007, **31**, 281.

9 J. H. Li, W. H. Lu, J. P. Ma and L. X. Chen, *Microchim. Acta*, 2011, **175**, 301.

10 A. R. Timerbaev, *Chem. Rev.*, 2013, **113**, 778.

11 L. Chen, T. T. Lou, C. W. Yu, Q. Kang and L. X. Chen, *Analyst*, 2011, **136**, 4770.

12 D. B. Liu, W. W. Chen, J. H. Wei, X. B. Li, Z. Wang and X. Y. Jiang, *Anal. Chem.*, 2012, **84**, 4185.

13 N. Zhou, J. H. Li, H. Chen, C. Y. Liao and L. X. Chen, *Analyst*, 2013, **138**, 1091.

14 A. E. Lanterna, E. A. Coronado and A. M. Granados, *J. Phys. Chem. C*, 2012, **116**, 6520.

15 X. Xue, F. Wang and X. Liu, *J. Am. Chem. Soc.*, 2008, **130**, 3244.

16 M. Rex, F. E. Hernandez and A. D. Campiglia, *Anal. Chem.*, 2006, **78**, 445.

17 T. T. Lou, Z. P. Chen, Y. Q. Wang and L. X. Chen, *ACS Appl. Mater. Interfaces*, 2011, **3**, 1568.

18 A. Campion and P. Kambhampati, *Chem. Soc. Rev.*, 1998, **27**, 241.

19 L. Guerrini and D. Graham, *Chem. Soc. Rev.*, 2012, **41**, 7085.

20 Y. Q. Wang, B. Yan and L. X. Chen, *Chem. Rev.*, 2013, **113**, 1391.

21 J. L. Li, L. X. Chen, T. T. Lou and Y. Q. Wang, *ACS Appl. Mater. Interfaces*, 2011, **3**, 3936.

22 Y. Y. Zhu, H. Kuang, L. G. Xu, W. Ma, C. F. Peng, Y. F. Hua, L. B. Wang and C. L. Xu, *J. Mater. Chem.*, 2012, **22**, 2387.

23 X. H. Jiang, Y. C. Lai, M. Yang, H. Yang, W. Jiang and J. H. Zhan, *Analyst*, 2012, **137**, 3995.

24 W. Ma, M. Z. Sun, L. G. Xu, L. B. Wang, H. Kuang and C. L. Xu, *Chem. Commun.*, 2013, **49**, 4989.

25 L. X. Chen, X. L. Fu and J. H. Li, *Nanoscale*, 2013, **5**, 5905.

26 G. Q. Wang and L. X. Chen, *Chin. Chem. Lett.*, 2009, **20**, 1475.

27 W. Ren, C. Zhu and E. Wang, *Nanoscale*, 2012, **4**, 5902.

28 H. S. Jung, K. Kim and M. S. Kim, *J. Mol. Struct.*, 1997, **407**, 139.

29 J. Hu, B. Zhao, W. Xu, B. Li and Y. Fan, *Spectrochim. Acta, Part A*, 2002, **58**, 2827.

30 B. Pergolese, M. Muniz-Miranda and A. Bigotto, *J. Phys. Chem. B*, 2004, **108**, 5698.

31 C. Y. Wu, W. Y. Lo, C. R. Chiu and T. S. Yang, *J. Raman Spectrosc.*, 2006, **37**, 799.

32 G. Wang, C. Lim, L. Chen, H. Chon, J. Choo, J. Hong and A. J. deMello, *Anal. Bioanal. Chem.*, 2009, **394**, 1827.

33 J. C. Fraire, L. A. Pérez and E. A. Coronado, *J. Phys. Chem. C*, 2013, **117**, 23090.

34 Y. F. Wang, Z. H. Sun, H. L. Hu, S. Y. Jing, B. Zhao, W. Q. Wu, C. Zhao and J. R. Lombardi, *J. Raman Spectrosc.*, 2007, **38**, 34.